Interface reaction of NiO/NiFe and its influence on magnetic properties

G. H. Yu,[a] C. L. Chai, F. W. Zhu, and J. M. Xiao
Department of Materials Physics, University of Science and Technology Beijing, Beijing, 100083, China

W. Y. Lai
Institute of Physics, Chinese Academy of Sciences, Beijing, 10080, China

(Received 25 August 2000; accepted for publication 28 November 2000)

Ta/NiO/NiFe/Ta multilayers were prepared by rf reactive and dc magnetron sputtering. The exchange coupling field between NiO and NiFe reached 120 Oe. The composition and chemical states at the interface region of NiO/NiFe were studied using the x-ray photoelectron spectroscopy (XPS) and peak decomposition technique. The results show that there are two thermodynamically favorable reactions at NiO/NiFe interface: $NiO+Fe=Ni+FeO$ and $3NiO+2Fe=3Ni+Fe_2O_3$. The thickness of the chemical reaction as estimated by angle-resolved XPS was about 1–1.5 nm. These interface reaction products are magnetic defects, and we believe that the exchange coupling field H_{ex} and the coercivity H_c of NiO/NiFe are affected by these defects. © *2001 American Institute of Physics.* [DOI: 10.1063/1.1343474]

''Exchange bias,'' [1] which refers to a shift (H_{ex}) in the magnetization curve away from the zero field axis is an important phenomenon observed when a ferromagnet (FM) is in contact with an antiferromagnet (AF). Despite four decades of research since its discovery, an understanding of this effect has still not been established. In recent years, the exchange coupling between ferromagnetic (FM) and antiferromagnetic (AF) thin films has received increasing attention in physics because it plays an important role in pinning the ferromagnetic layer in giant magnetoresistance heads or spin valves.[2,3] Consequently, this promotes afresh the study of the exchange coupling mechanism.

The simplest theory explained the effect in terms of an uncompensated monolayer of spins at the surface of the antiferromagnetic layer.[4] However, this model predicts an H_{ex} 100 times greater than that observed in experiment.[5] Recently, several theories have given improved predictions of the size of H_{ex}, but do not agree on a physical explanation of the effect. Malozemoff assumed the formation of AF domains perpendicular to the interface plane due to the random field created by roughness.[5] Mauri *et al.* proposed a subsequent model with the formation of AF domains parallel to the interface when the FM layer rotates.[6] Koon performed calculations indicating a 90° or ''spin flop'' coupling between the AF and FM layers, which correctly predicted the magnitude of H_{ex}.[7] However, the sign of the bias was not definitely determined. This was recently addressed by Hong.[8] Note that spin flop coupling can occur only for antiferromagnetic layers with an alternating 180° spin structure. At present, acquiring details of mirostructure at the AF/FM interface in real materials is useful for testing the present models and even proposing a new model.

Up to now, the antiferromagnetic materials used in spin valve multilayer with giant magnetoresistance have been Mn alloys—XMn ($X=$Fe, Ni, Ir, Pt, Pd etc.), CoO and NiO mainly. The advantages of NiO are superior corrosion resistance, relatively high blocking temperature, and high resistivity. It has been used in spin valve multilayers.[9] Its disadvantage is its weaker exchange coupling (H_{ex}). In order to increase the H_{ex}, extensive studies have been done. The factors studied which could influence the H_{ex} of NiO/NiFe are (1) interfacial roughness[10] and its slopes,[9] (2) interfacial atoms interdiffusion,[11] and (3) the texture[10] and grain size[12] of AF thin films. In this letter, the mirostructure of NiO/NiFe interface was studied using x-ray photoelectron spectroscopy (XPS). We report a mechanism producing magnetic defects at the interface—i.e., an interfacial chemical reaction of NiO/NiFe. The effects of magnetic defects on the exchange coupling field (H_{ex}) and coercivity H_c in the NiO/NiFe system are discussed.

Samples were prepared in magnetron sputtering systems. Ta(12 nm)/NiO(50 nm)/$Ni_{81}Fe_{19}$(7 nm)/Ta(9 nm) were deposited on glass substrates in regular order. The base pressure was less than 4×10^{-5} Pa and the argon sputtering pressure was 0.5 Pa. The substrates were cooled by water. A permanent magnet which produced a magnetic field of ~250 Oe along the substrate surface was present during the deposition process. This field produced an easy axis in the NiFe film and defined the exchange-coupling axis. NiO was obtained by rf reactive sputtering in the mixed atmosphere of Ar and O_2. The ratio of Ar to O_2 was controlled through mass flow controllers and adjusted by the chemical states of nickel or stoichiometries of Ni and O gained from XPS in order to produce pure NiO without metallic Ni and Ni^{3+}. The hysteresis loops were obtained from a JDJ9600 vibrating sample magnetometer. The exchange coupling field (H_{ex}) and coercivity (H_c) in NiO/NiFe films could be obtained from the hysteresis loops.

For XPS analysis, Ta(12 nm)/NiO(50 nm)/$Ni_{81}Fe_{19}$(3 nm)/Ta(3 nm) layers were fabricated in the same way as the Ta(12 nm)/NiO(50 nm)/$Ni_{81}Fe_{19}$(7 nm)/Ta(9 nm) layers. The samples were introduced into a MICROLAB MK II x-ray photoelectron spectroscopy system instantly after being taken out of the deposition system. The vacuum of the analysis chamber was less than 3×10^{-7} Pa. An Al $K\alpha$ line at 1486.6 eV was used with the x-ray source run at 14.5 kV.

[a]Electronic mail: guanghua-yu@263.net

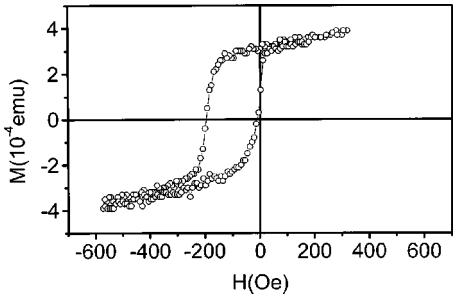

FIG. 1. Hysteresis loop of Ta(12 nm)/NiO(50 nm)/NiFe(7 nm)/Ta(9 nm).

The energy analyzer was operated at a constant pass energy of 50 eV. First, the samples were sputter cleaned by lower energy Ar^+ to remove the Ta protective layer (The sputter rate of Ar^+ to Ta protective layer had been accurately calibrated). The Ar^+ gun was operated at 0.5 kV at a pressure of 1×10^{-4} Pa, and the Ar^+ ion current density was 50 μA/cm^2. Simultaneously, XPS data were received by using a 5° takeoff angle for photoelectrons with respect to the samples surface plane to monitor the appearance of the $Ni_{81}Fe_{19}$ layer. Then, angle-resolved XPS was used to study different depth information of the $Ni_{81}Fe_{19}$. In order to detect the composition and chemical states at the NiO/NiFe interface using x-ray photoelectron spectroscopy, the interfacial layer has to be within the XPS detectable sampling depth $d=3\lambda\sin\alpha$,[13] where λ and α are inelastic mean-free paths (IMFPs) for photoelectrons and a takeoff angle for photoelectrons with respect to the samples surface plane, respectively.[13] About 95% of the total photoelectron signal will arise from this sampling depth. The IMFPs can be obtained by using the table compiled by Tanuma *et al.*[14] For an Al $K\alpha$ radiation source, the IMFPs for Fe $2p$ in Fe and for Ni $2p$ in Ni are 13.4 and 10.7 Å, respectively. The IMFPs for Fe $2p$ and Ni $2p$ in their oxidates are about 1–2 Å more than those in Fe and Ni, respectively. When $\alpha=90°$ the detectable depth $d=3\lambda$, i.e., the signal from the NiO/NiFe interface can be detected. All binding energies have been corrected for the sample charging effect with reference to the C $1s$ line at 284.6 eV. The XPS peak areas and peak decomposition (i.e., ''curve fitting'') were determined using Gaussian(80%)–Lorentzian(20%) curve fitting software (including the atomic sensitivity factor) provided by this XPS system. Peak areas were measured with a precision of 5% or better.

Figure 1 shows the hysteresis loop of Ta(12 nm)/NiO(50 nm)/$Ni_{81}Fe_{19}$(7 nm)/Ta(9 nm). From the hysteresis loop the exchange coupling field H_{ex} (120 Oe) and coercivity H_c (110 Oe) can be obtained. The results correspond to what Lin *et al.*[15] reported. Hwang *et al.*[9] got the exchange coupling field H_{ex} ($\sim$90 Oe) and coercivity H_c ($\sim$90 Oe) at NiFe thickness of 5 nm using Si_3N_4 as a buffer layer. This is also approximate to our experiment results.

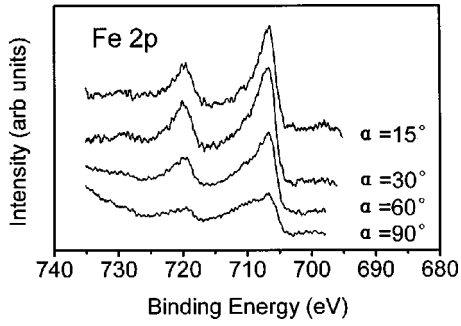

FIG. 2. Fe $2p$ high-resolution XPS spectra obtained near NiO/NiFe interface for $\alpha=15°$, 30°, 60°, and 90°, α is a takeoff angle for photoelectrons with respect to the samples surface plane.

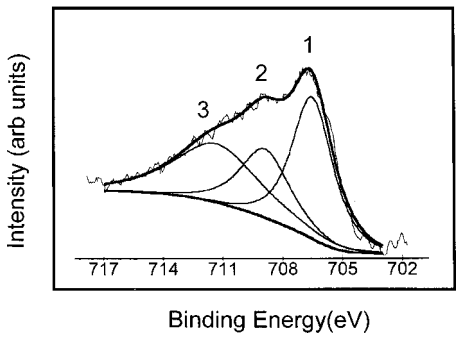

FIG. 3. Computer fitting curve of Fe $2p_{3/2}$ high-resolution XPS spectrum for $\alpha=90°$.

Angle-resolved XPS was used to study the $Ni_{81}Fe_{19}$ layer after having sputter cleaned the Ta protective layer of sample glass/Ta(12 nm)/NiO(50 nm)/NiFe(3 nm)/Ta(3 nm), and the spectra of iron and nickel acquired were fitted by the above mentioned curve fitting software to determine the atomic fraction of iron and nickel in all chemical states. Figure 2 shows Fe$2p$ high-resolution XPS spectra obtained for the takeoff angle for photoelectrons with respect to the samples surface plane $\alpha=15°$, 30°, 60° and 90°. The Fe $2p$ high-resolution XPS spectra broaden with increasing detectable sampling depth. This indicated iron existed in different chemical states. Since the detectable depth $d=3\lambda\sin\alpha$, the XPS Spectrum with $\alpha=90°$ included the signals from NiO/NiFe Interface. Figure 3 represents a computer fitted curve of a Fe $2p_{3/2}$ high-resolution XPS spectrum for $\alpha=90$, it can actually be fitted with three components. From the XPS handbook,[16] we know that peak 1 at 706.60 eV is characteristic of a metallic Fe $2p_{3/2}$ peak, peak 2 at 709.00 eV and peak 3 at 711.30 eV correspond to $Fe^{2+}2p_{3/2}$ and $Fe^{3+}2p_{3/2}$ peaks, respectively. From the area of three fitted curves the mean percentage of Fe, Fe^{2+}, and Fe^{3+} within the detectable depth could be evaluated and is 41%, 24%, and 35%, respectively. Figure 4 shows Ni $2p$ high-resolution XPS spectra obtained for different α—only the Ni $2p$ high-resolution XPS spectrum for $\alpha=90°$ broadens. Figure 5 represents a computer fitted curve of a Ni $2p$ high-resolution XPS spec-

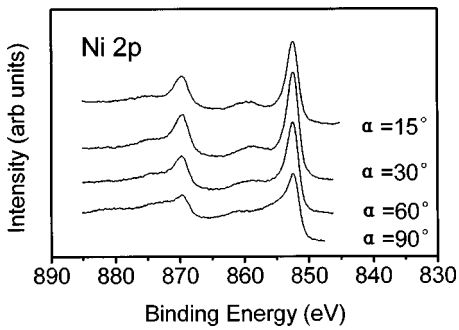

FIG. 4. Ni $2p$ high-resolution XPS spectra obtained near NiO/NiFe interface for $\alpha=15°$, 30°, 60°, and 90°.

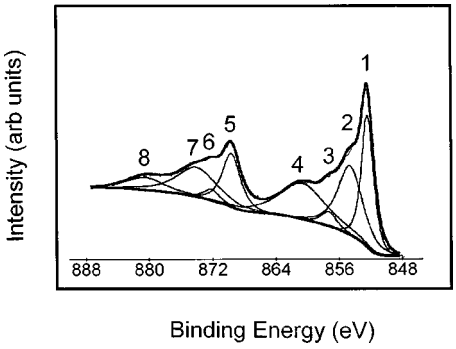

FIG. 5. Computer fitting curve of Ni $2p$ high-resolution XPS spectrum for $\alpha=90°$.

trum for $\alpha=90°$, it can actually be fitted with eight peaks. From the XPS handbook,[16] we know that peak 1 at 852.30 eV and peak 5 at 869.60 eV are characteristic of metallic Ni $2p_{3/2}$ and Ni $2p_{1/2}$ peaks, respectively, peak 3 and peak 6 are accompanying peaks; peak 2 at 854.50 eV and peak 7 at 874.00 eV correspond to $Ni^{2+}2p_{3/2}$ and $Ni^{2+}2p_{1/2}$ peaks, respectively, peak 4 and peak 8 are accompanying peaks. Fitting results indicate the mean percentages of Ni and Ni^{2+} within the detectable depth are 62% and 38%, respectively. Further, estimation indicates that $Ni_{81}Fe_{19}$ has changed to $Ni_{1-x}Fe_x$ ($x\leqslant 8$ at. %) from fitting results of Figs. 3 and 5.

The iron oxides could not be found during the sample preparation because we pumped the chamber back to a base pressure of 4×10^{-5} Pa after the deposition of NiO film and presputtered the NiFe target for 30 min before the deposition of NiFe film. The existence of Fe^{2+} and Fe^{3+} near the NiO/NiFe interface can be understood by considering the reaction: NiO+Fe=Ni+FeO and $3NiO+2Fe=3Ni+Fe_2O_3$. The Gibbs free-energy change in the reactions is about -33.3 and -108.9 KJ/mol,[17] which means that both reactions are thermodynamically favorable. The formation enthalpy ΔH of NiO is 2.5 eV. The atoms which had been sputtered off from the target and arrived at the substrate were provided with kinetic energy of about several to tens of electron volts.[18] Therefore, the reactions are dynamically possible. The above results show that during the deposition process, the NiFe and NiO layers are intermixed together, with the Fe atoms grabbing O from NiO and forming FeO and Fe_2O_3. From Fig. 2 we can see the Fe $2p_{3/2}$ high-resolution XPS spectrum gradually broaden starting from $\alpha=30°$. The XPS detectable sampling depth at $\alpha=30°$ can be calculated by $d=3\lambda\sin\alpha$, and the thickness of NiFe layer is 3 nm. Thus, the thickness of the chemical reaction is to be estimated at about 1–1.5 nm.

The results of XPS indicate that there are defects (FeO and Fe_2O_3) forming near the NiO/NiFe interface. Thus, actual contact areas of NiFe with NiO greatly diminish, and the defects also hinder domain walls in NiFe layer from moving. We believe that the former leads to a decrease in the exchange coupling field H_{ex}, and the latter gives rise to an increase in the coercivity H_c. The analysis of XPS gives definite composition of defects. FeO and Fe_2O_3 may form ferrite with a lower Curie temperature, and the decrease of Fe fraction in the NiFe film at the interface also leads to the reduction of the Curie temperature and magnetic moments of the NiFe film. These magnetic defects could cause magnetic fluctuation near the interface, which would have an effect on H_{ex} and H_c.

In view of the angle-resolved XPS analysis of the NiO/NiFe interface, we report the evidence of chemical reactions which took place at NiO/NiFe interface: NiO+Fe=Ni+FeO and $3NiO+2Fe=3Ni+Fe_2O_3$. FeO and Fe_2O_3 formed at the NiO/NiFe interface led to the weaker exchange coupling field and the higher coercivity of NiO/NiFe films. It is obvious that the interface chemical reaction is an important factor influencing exchange coupling.

The authors would like to thank the National Science Foundation of China for their support under Grant No. 19890310.

[1] W. H. Meiklejohn and C. P. Bean, Phys. Rev. **102**, 1423 (1956).
[2] M. J. Carey and A. E. Berkowitz, Appl. Phys. Lett. **60**, 3060 (1992).
[3] S. S. P. Parkin and V. R. Deline, Phys. Rev. B **42**, 10 583 (1990).
[4] W. H. Meiklejohn and C. P. Bean, Phys. Rev. **105**, 904 (1957).
[5] A. P. Malozemoff, Phys. Rev. B **35**, 3679 (1987); **37**, 7673 (1988).
[6] D. Mauri, H. C. Siegemann, P. S. Bagus, and E. Kay, J. Appl. Phys. **62**, 3047 (1987).
[7] N. C. Koon, Phys. Rev. Lett. **78**, 4865 (1997).
[8] T. M. Hong, Phys. Rev. B **58**, 97 (1998).
[9] D. G. Hwang, S. S. Lee, and C. M. Park, Appl. Phys. Lett. **72**, 2162 (1998).
[10] J. X. Shen and M. T. Kief, J. Appl. Phys. **79**, 5008 (1996).
[11] Z. H. Qian and J. M. Sivertsen, J. Appl. Phys. **83**, 6825 (1998).
[12] C. H. Lai, T. C. Anthony, E. Iwamura, and P. L. White, IEEE Trans. Magn. **32**, 3419 (1996).
[13] E. Atanassova, T. Dimitrova, and J. Koprinarova, Appl. Surf. Sci. **84**, 193 (1995).
[14] S. Tanuma, C. J. Powell, and D. R. Penn, Surf. Interface Anal. **11**, 577 (1988).
[15] T. Lin, C. Tsang, R. E. Fontana, and J. K. Howard, IEEE Trans. Magn. **31**, 2585 (1995).
[16] C. D. Wagner, W. M. Riggs, L. E. Davis, and J. F. Moulder, *Handbook of X-ray Photoelectron Spectroscopy* (Perkin-Elmer, 1979), pp. 81 and 144.
[17] O. Kubaschewski, C. B. Alcock, and P. J. Spencer, *Materials Theromochemistrys* (Pergamon, New York, 1993), pp. 278 and 300.
[18] J. C. S. Kools, J. Appl. Phys. **77**, 2993 (1995).